INTERNATIONAL JOURNAL FOR NUMERICAL METHODS IN FLUIDS, VOL. 15, 571–578 (1992)

A FINITE ELEMENT METHOD FOR A THREE-DIMENSIONAL SECOND-ORDER CLOSURE MODEL OF TURBULENT DIFFUSION IN A CONVECTIVE BOUNDARY LAYER

PRASAD PAI* AND TATE T. H. TSANG†

Department of Chemical Engineering, University of Kentucky, Lexington, KY 40506-0046, U.S.A.

SUMMARY

A three-dimensional second-order closure dispersion model is used to simulate the plume behaviour of a passive contaminant in a convective boundary layer. A time-splitting finite element method together with a non-linear filtering scheme is used to solve the three-dimensional second-order closure transport equations. The model results show good agreement with laboratory data for a ground level source.

KEY WORDS Three-dimensional second-order closure model Convective boundary layers Plume behaviour Time-splitting finite element method

INTRODUCTION

The pioneering laboratory convection tank experiments by Deardorff and Willis[1] and Willis and Deardorff[2–4] showed that plume dispersion in convective boundary layers depends on the source height. For the case of near-ground emissions the plume 'lifts off' from the ground and forms an elevated maximum concentration close to the inversion layer. For the case of elevated sources the plume 'descends' and forms a local ground level maximum at a certain downwind distance. Wind tunnel experiments[5] and field data[6] further confirmed the laboratory results. This unusual behaviour of plume dispersion is due to the skewness of the vertical velocity in convective boundary layers.[7,8]

Recent Eulerian modelling attempts of atmospheric diffusion have been using the higher-order closure approach. Today, second-order closure models are the only time-averaging models that can describe the turbulent diffusion in convective boundary layers.[9–14] The main advantage with the second-order closure approach is that it incorporates the physics of the dispersion problem in much greater detail than the commonly used Gaussian plume model and the K-diffusion (eddy diffusivity) model. However, second-order closure dispersion models contain more differential equations than K-diffusion models. Therefore second-order closure models require more CPU time and storage. This seriously limits their repeated use for practical applications. In order to develop practical second-order closure dispersion models, we need to consider the following two

* Present address: ENSR Consulting and Engineering, 1220 Avenida Acaso, Camarill, CA 93012, U.S.A.
† Author to whom correspondence should be addressed.

0271–2091/92/170571–08$09.00

Received 10 July 1991
Revised 15 January 1992

factors: (a) the parametrization of higher-order terms must be simple, yet capable of capturing the essential plume behaviour; (b) the numerical algorithm must have a fast turnaround time. These two factors have guided our present work of developing a three-dimensional second-order closure dispersion model to predict mean pollutant concentration in convective boundary layers.

Currently, there is limited work on three-dimensional second-order closure modelling of turbulent diffusion, although recent preliminary results from two-dimensional studies are very promising.[9-12] Earlier work by Lewellen and Teske[13] showed that their second-order closure model could predict a rather weak plume 'lift-off' phenomenon (without an elevated local maximum) for a near-ground source. More recently, Enger[14] used a second-order closure model to simulate dispersion from a point source in unstable and stable conditions. In Enger's model the scalar/pressure gradient covariance is parametrized according to Lumley[15] and the third-order correlation is modelled by a gradient diffusion approximation. However, the plume 'lift-off' and 'descending' phenomena were not shown.

In this paper, Donaldson's[16] model is used for the parametrization of scalar/pressure gradient covariance terms and third-order correlations. We demonstrate that Donaldson's model can describe the plume behaviour in convective boundary layers. Furthermore, we show how the time-splitting finite element method reduces a three-dimensional problem to a sequence of locally one-dimensional problems, thus avoiding the numerical solution of an extremely large sparse matrix system for each time step.

SECOND-ORDER CLOSURE MODEL EQUATIONS

Consider the transient dispersion of a passive contaminant from a point source in a horizontally homogeneous convective boundary layer. The three-dimensional ensemble-averaged transport equation describing this process is

$$\frac{\partial C}{\partial t}+U\frac{\partial C}{\partial x}+V\frac{\partial C}{\partial y}=\frac{\partial(-\overline{uc})}{\partial x}+\frac{\partial(-\overline{vc})}{\partial y}+\frac{\partial(-\overline{wc})}{\partial z}, \tag{1}$$

where C is the mean concentration, U and V are the mean wind velocity components in the x- and y-directions respectively and $\overline{uc}$, $\overline{vc}$ and $\overline{wc}$ are the turbulent fluxes in the x-, y- and z-directions respectively. In order to solve this equation, we have to know the turbulent fluxes. We will therefore introduce the three-dimensional ensemble-averaged transport equations for $\overline{uc}$, $\overline{vc}$ and $\overline{wc}$. In the transport equations for the turbulent fluxes, several higher-order terms must be modelled. The following guidelines, based on Donaldson's model, are used in the modelling of various correlation terms: (a) the molecular terms are neglected in comparison with the other terms of the equation; (b) the third-order velocity correlation is modelled using the gradient diffusion approximation; (c) the pressure gradient–velocity correlation is decomposed into a pressure diffusion term and a tendency-towards-isotropy term; (d) the dissipation terms are modelled by assuming that the small-scale turbulence structure is isotropic; (e) only the vertical transport terms are retained in the equations for the second-order correlations. With the assumption of horizontal homogeneity in the mean flow variables, Reynolds stresses and turbulent heat fluxes, we can write transport equations for the three components of turbulent mass fluxes as

$$\frac{\partial\overline{uc}}{\partial t}+U\frac{\partial\overline{uc}}{\partial x}+V\frac{\partial\overline{uc}}{\partial y}=-\overline{uu}\frac{\partial C}{\partial x}-\overline{uv}\frac{\partial C}{\partial y}-\overline{uw}\frac{\partial C}{\partial z}-\overline{wc}\frac{\partial U}{\partial z}+\frac{\partial}{\partial z}\left(\Lambda_2 q\frac{\partial\overline{uc}}{\partial z}\right)-\left(\frac{Aq}{\Lambda}\right)\overline{uc}, \tag{2}$$

$$\frac{\partial\overline{vc}}{\partial t}+U\frac{\partial\overline{vc}}{\partial x}+V\frac{\partial\overline{vc}}{\partial y}=-\overline{uv}\frac{\partial C}{\partial x}-\overline{vv}\frac{\partial C}{\partial y}-\overline{vw}\frac{\partial C}{\partial z}-\overline{wc}\frac{\partial V}{\partial z}+\frac{\partial}{\partial z}\left(\Lambda_2 q\frac{\partial\overline{vc}}{\partial z}\right)-\left(\frac{Aq}{\Lambda}\right)\overline{vc}, \tag{3}$$

$$\frac{\partial \overline{wc}}{\partial t}+U\frac{\partial \overline{wc}}{\partial x}+V\frac{\partial \overline{wc}}{\partial y}=-\overline{uw}\frac{\partial C}{\partial x}-\overline{vw}\frac{\partial C}{\partial y}-\overline{ww}\frac{\partial C}{\partial z}+\overline{c\theta}\left(\frac{g}{\Theta_0}\right)$$
$$+\frac{\partial}{\partial z}\left(2\Lambda_2 q\frac{\partial \overline{wc}}{\partial z}\right)+\frac{\partial}{\partial z}\left(\Lambda_3 q\frac{\partial \overline{wc}}{\partial z}\right)-\left(\frac{Aq}{\Lambda}\right)\overline{wc}. \tag{4}$$

The equation for the vertical turbulent flux $\overline{wc}$ introduces the covariance of concentration and temperature, $\overline{c\theta}$. Since it is a second-order moment, we must write a transport equation for $\overline{c\theta}$. Treating the terms in the equation for the covariance $\overline{c\theta}$ in a way similar to the turbulent mass fluxes, we get

$$\frac{\partial \overline{c\theta}}{\partial t}+U\frac{\partial \overline{c\theta}}{\partial x}+V\frac{\partial \overline{c\theta}}{\partial y}=-\overline{u\theta}\frac{\partial C}{\partial x}-\overline{v\theta}\frac{\partial C}{\partial y}-\overline{w\theta}\frac{\partial C}{\partial z}-\overline{wc}\frac{\partial \Theta}{\partial z}+\frac{\partial}{\partial z}\left(\Lambda_2 q\frac{\partial \overline{c\theta}}{\partial z}\right)-\left(\frac{2bsq}{\Lambda}\right)\overline{c\theta}. \tag{5}$$

In equations (2)–(5), $q\ (=\overline{u_i u_i}^{1/2})$ is the turbulent velocity, $\overline{u_i u_j}$ is the Reynolds stress tensor, $\overline{u_i\theta}$ are the components of the heat flux and g is the acceleration due to gravity. The length scales Λ, Λ_2 and Λ_3 are due to modelling of the higher-order terms. A, b and s are model constants. The choice of length scales and model constants will be discussed later.

The left-hand sides of equations (1)–(5) contain the temporal derivatives and the advection terms of the five unknown variables. The first four terms on the right-hand side of equations (2), (3) and (5) and the first three terms on the right-hand side of equation (4) are the production terms. The fourth term on the right-hand side of equation (4) is the buoyancy production term. The fifth terms on the right-hand side of equations (2)–(5) are the results of parametrizing the gradients of third-order correlations. The sixth term on the right-hand side of equation (4) is the approximation of the pressure diffusion term. Since we have retained only the vertical transport terms, the pressure diffusion term does not appear in equations (2), (3) and (5). The last terms on the right-hand side of equations (2)–(4) are model representations of the tendency-towards-isotropy term. The last term on the right-hand side of equation (5) is the parametrization of the dissipation term for the covariance of concentration and temperature.

A Gaussian distribution for C was used as the boundary condition to approximate the point source:

$$C(\bar{x}, y, z)=\frac{Q}{2\pi\sigma_y(\bar{x})\,\sigma_z(\bar{x})\,U_m}\exp\left(\frac{-y^2}{2\sigma_y^2(\bar{x})}\right)\left[\exp\left(\frac{-(z_s-z)^2}{2\sigma_z^2(\bar{x})}\right)+\exp\left(\frac{-(z_s+z)^2}{2\sigma_z^2(\bar{x})}\right)\right], \tag{6}$$

where $\bar{x}$ is the downwind distance at which the boundary condition is applied. This is done to avoid singularity at $x=0$. Thus the values of the concentration calculated by equation (6) for a point source projected at $C(\bar{x}=300\text{ m}, y=0, z=z_s)$ are the boundary values for the simulation. The horizontal and vertical standard deviations $\sigma_y(\bar{x})$ and $\sigma_z(\bar{x})$ respectively at a distance $\bar{x}$ are obtained from Willis and Deardorff.[2–4] At the top of the boundary layer we have used the following boundary conditions:

$$\frac{\partial C}{\partial z}=0, \qquad \overline{uc}=0, \qquad \overline{vc}=0, \qquad \frac{\partial \overline{wc}}{\partial z}=0, \qquad \overline{c\theta}=0. \tag{7}$$

At the surface the boundary conditions are

$$\frac{\partial C}{\partial z}=0, \qquad \frac{\partial \overline{uc}}{\partial z}=0, \qquad \frac{\partial \overline{vc}}{\partial z}=0, \qquad \overline{wc}=0, \qquad \frac{\partial \overline{c\theta}}{\partial z}=0. \tag{8}$$

The length scale Λ is obtained from Sun:[10]

$$\Lambda = 0{\cdot}25\{1{\cdot}8\, z_i[1-\exp(-4z/z_i)-0{\cdot}0003\exp(8z/z_i)]\} \tag{9}$$

for unstable stratification and

$$\Lambda = \begin{cases} 0{\cdot}76[E/(g/\Theta)(\mathrm{d}\theta/\mathrm{d}z)]^{1/2}, & \Lambda \leqslant \Delta z \\ \Delta z, & \Lambda > \Delta z \end{cases} \tag{10}$$

for stable stratification, where z_i is the inversion height, z is the vertical height and Δz is the grid size in the vertical direction. The other length scales are specified as

$$\Lambda_2 = c_2\Lambda, \tag{11}$$

$$\Lambda_3 = c_3\Lambda. \tag{12}$$

The values of the constants $A=0{\cdot}75$, $b=0{\cdot}125$, $s=1{\cdot}8$, $c_2=0{\cdot}3$ and $c_3=-0{\cdot}3$ are based on Lewellen and Teske's second-order closure model.[17]

A TIME-SPLITTING FINITE ELEMENT METHOD

The Galerkin finite element method with linear basis function and its variants such as Taylor–Galerkin and Petrov–Galerkin methods are commonly used in air pollution modelling.[18–20] For convective transport the Galerkin finite element method retains the peak value of the concentration distribution very well and requires less CPU time and minimal memory storage. However, the use of formal finite element methods for equations (1)–(5) requires numerical solutions of a large sparse matrix for each time step. For such a three-dimensional problem the number of unknowns is often of the order of 10^5–10^6. Currently, numerical solutions of such a large matrix system prove to be difficult and challenging. Therefore we use a time-splitting technique to reduce the three-dimensional problem to the following three locally one-dimensional problems.

X-direction equations

$$\frac{\partial C}{\partial t} + U\frac{\partial C}{\partial x} = \frac{\partial(-\overline{uc})}{\partial x)}, \tag{13}$$

$$\frac{\partial \overline{uc}}{\partial t} + U\frac{\partial \overline{uc}}{\partial x} = -\overline{uu}\frac{\partial C}{\partial x} - \frac{1}{3}\overline{wc}\frac{\partial U}{\partial z} - \frac{1}{3}\left(\frac{Aq}{\Lambda}\right)\overline{uc}, \tag{14}$$

$$\frac{\partial \overline{vc}}{\partial t} + U\frac{\partial \overline{vc}}{\partial x} = -\overline{uv}\frac{\partial C}{\partial x} - \frac{1}{3}\overline{wc}\frac{\partial V}{\partial z} - \frac{1}{3}\left(\frac{Aq}{\Lambda}\right)\overline{vc}, \tag{15}$$

$$\frac{\partial \overline{wc}}{\partial t} + U\frac{\partial \overline{wc}}{\partial x} = -\overline{uw}\frac{\partial C}{\partial x} + \frac{1}{3}\overline{c\theta}\left(\frac{g}{\Theta_0}\right) - \frac{1}{3}\left(\frac{Aq}{\Lambda}\right)\overline{wc}, \tag{16}$$

$$\frac{\partial \overline{c\theta}}{\partial t} + U\frac{\partial \overline{c\theta}}{\partial x} = -\overline{u\theta}\frac{\partial C}{\partial x} - \frac{1}{3}\overline{wc}\frac{\partial \Theta}{\partial z} - \frac{1}{3}\left(\frac{2bsq}{\Lambda}\right)\overline{c\theta}. \tag{17}$$

Y-direction equations

$$\frac{\partial C}{\partial t}+V\frac{\partial C}{\partial y}=\frac{\partial(-\overline{vc})}{\partial y}, \tag{18}$$

$$\frac{\partial \overline{uc}}{\partial t}+V\frac{\partial \overline{uc}}{\partial y}=-\overline{uv}\frac{\partial C}{\partial y}-\frac{1}{3}\overline{wc}\frac{\partial U}{\partial z}-\frac{1}{3}\left(\frac{Aq}{\Lambda}\right)\overline{uc}, \tag{19}$$

$$\frac{\partial \overline{vc}}{\partial t}+V\frac{\partial \overline{vc}}{\partial y}=-\overline{vv}\frac{\partial C}{\partial y}-\frac{1}{3}\overline{wc}\frac{\partial V}{\partial z}-\frac{1}{3}\left(\frac{Aq}{\Lambda}\right)\overline{vc}, \tag{20}$$

$$\frac{\partial \overline{wc}}{\partial t}+V\frac{\partial \overline{wc}}{\partial y}=-\overline{vw}\frac{\partial C}{\partial y}+\frac{1}{3}\overline{c\theta}\left(\frac{g}{\Theta_0}\right)-\frac{1}{3}\left(\frac{Aq}{\Lambda}\right)\overline{wc}, \tag{21}$$

$$\frac{\partial \overline{c\theta}}{\partial t}+V\frac{\partial \overline{c\theta}}{\partial y}=-\overline{v\theta}\frac{\partial C}{\partial y}-\frac{1}{3}\overline{wc}\frac{\partial \Theta}{\partial z}-\frac{1}{3}\left(\frac{2bsq}{\Lambda}\right)\overline{c\theta}. \tag{22}$$

Z-direction equations

$$\frac{\partial C}{\partial t}=\frac{\partial(-\overline{wc})}{\partial z}, \tag{23}$$

$$\frac{\partial \overline{uc}}{\partial t}=-\overline{uw}\frac{\partial C}{\partial z}+\frac{\partial}{\partial z}\left(\Lambda_2 q\frac{\partial \overline{uc}}{\partial z}\right)-\frac{1}{3}\overline{wc}\frac{\partial U}{\partial z}-\frac{1}{3}\left(\frac{Aq}{\Lambda}\right)\overline{uc}, \tag{24}$$

$$\frac{\partial \overline{vc}}{\partial t}=-\overline{vw}\frac{\partial C}{\partial z}+\frac{\partial}{\partial z}\left(\Lambda_2 q\frac{\partial \overline{vc}}{\partial z}\right)-\frac{1}{3}\overline{wc}\frac{\partial V}{\partial z}-\frac{1}{3}\left(\frac{Aq}{\Lambda}\right)\overline{vc}, \tag{25}$$

$$\frac{\partial \overline{wc}}{\partial t}=-\overline{ww}\frac{\partial C}{\partial z}+\frac{\partial}{\partial z}\left(\Lambda_2 q\frac{\partial \overline{wc}}{\partial z}\right)+\frac{1}{3}\overline{c\theta}\left(\frac{g}{\Theta_0}\right)-\frac{1}{3}\left(\frac{Aq}{\Lambda}\right)\overline{wc}, \tag{26}$$

$$\frac{\partial \overline{c\theta}}{\partial t}=-\overline{w\theta}\frac{\partial C}{\partial z}+\frac{\partial}{\partial z}\left(\Lambda_2 q\frac{\partial \overline{c\theta}}{\partial z}\right)-\frac{1}{3}\overline{wc}\frac{\partial \Theta}{\partial z}-\frac{1}{3}\left(\frac{2bsq}{\Lambda}\right)\overline{c\theta}. \tag{27}$$

Equations (13)–(17), (18)–(22) and (23)–(27) are the governing transport equations for C, $\overline{uc}$, $\overline{vc}$, $\overline{wc}$ and $\overline{c\theta}$ in the x-, y- and z-directions respectively. The three sets of equations were solved sequentially and the five equations within each set were solved simultaneously.

The Crank–Nicolson scheme and the Galerkin finite element method with linear basis function are used to discretize equations (13)–(27). The resulting block tridiagonal systems are solved by TRIDBLOK, an implementation of the standard block tridiagonal system solver at the University of Kentucky. To improve the performance on the IBM 3090-600J, we have also used the vector versions of the ESSL subroutines DGBF and DGBS (ESSL is the Engineering and Scientific Subroutine Library by IBM).

It is well known that use of the Galerkin finite element method with linear basis function for convective diffusion equations creates negative concentrations in regions of sharp gradients. These negative concentrations are erroneous and lead to numerical instability for chemical reactive flows in air pollution modelling. Therefore it is desirable to use a filter which removes negative values of concentration without significantly affecting the filtered function. A popular filtering technique is to set the negative concentrations to zero at each time step. However, this

type of filtering procedure does not conserve the total mass. We have used a simple non-linear filter[21] which completely eliminates the negative concentration, conserves the total mass and retains the maxima and shape of the concentration field relatively close to the original. Bartinicki[21] applied the filter to numerical solutions of the advection equation calculated by a pseudospectral method. Here we apply the filter to the time-splitting finite element method. It suffices to say that the filtering scheme works satisfactorily for equations (13)–(27).

RESULTS AND DISCUSSION

The grid system used in the present study has 39 grid points in the x- and y-directions with $\Delta x = \Delta y = 100$ m and 53 grid points in the vertical direction with $\Delta z = 25$ m. The three-dimentsional time-splitting finite element method determines five unknowns per grid point per time step, which amounts to approximately 403 000 unknowns per time step. We have used $\Delta t = 2$ s for all simulations, with the steady state simulation requiring 1000 times steps. The mean variables U, V and Θ and the turbulence fields of meteorological variables, which include $\overline{u_i u_j}$ and $\overline{u_i \theta}$, are obtained from Wyngaard and Cote[22] at 14:00 EST during day 33 of Wangara experiments and serve as inputs to the three-dimensional diffusion model, equations (1)–(5). The x-direction in Wyngaard and Cote's[22] model is aligned along the surface layer wind direction, which shows a much larger x-component ($U_m \approx 2{\cdot}2$ m s^{-1}) of the mean wind in the bulk of the mixed layer. The y-component is almost negligible except at the top of the mixed layer. The results of simulations are expressed in terms of dimensionless variables defined by $C^* = Cz_i^2 U_m/Q$, $X = xw_*/U_m z_i$, $Y = y/z_i$ and $Z = z/z_i$, where C^*, X, Y and Z are the dimensionless concentration, downwind distance, cross-wind distance and vertical height respectively. U_m is the mean wind speed in the convective boundary layer, w_* is the convective velocity scale, z_i is the inversion height and Q is the source strength. The convective velocity scale is given by $w_* = (\alpha g H_0 z_i)^{1/3}$, where α is the coefficient of thermal expansion and H_0 is the kinematic heat flux near the surface. At 14:00 EST Wangara day 33 the convective boundary layer was fully developed with $z_i = 1100$ m.

Figure 1 compares the dimensionless cross-wind integrated concentration obtained from the laboratory experiments of Willis and Deardorff[2] and the second-order closure model for a near-ground source, $z_s/z_i = 0{\cdot}067$ ($z_s = 75$ m). The dimensionless cross-wind integrated concentration is defined by

$$C_y^* = \int_{-\infty}^{\infty} C^*(X, Y, Z)\mathrm{d}Y. \tag{28}$$

The second-order closure model predicts an elevated concentration maximum at a height of about $Z = 0{\cdot}9$ near $X = 2{\cdot}0$. The location of the elevated maximum from the laboratory experiments ($Z = 0{\cdot}8$, $X = 1{\cdot}5$) differs from the simulated results as seen in Figure. 1. This could be due to the treatment of the overlying stable boundary layer above inversion. Furthermore, in the laboratory experiments[2-4] there is no mean wind present, but the results are presented in terms of a uniform mean wind along the x-axis by using Taylor's hypothesis. Willis and Deardorff[23] showed that the Taylor hypothesis is valid and streamwise diffusion is negligible if the ratio U_m/w_* is greater than 1·2. It should be mentioned that even at this lower limit of 1·2 the streamwise diffusion effect was rarely observed in their experiments. In our simulations the ratio U_m/w_* is 1·1 which is close enough for justifiably neglecting the diffusion terms. Furthermore, Enger[14] shows that there is very little difference in the result if the horizontal transport terms (i.e. horizontal gradients of third-order correlations, which give rise to horizontal diffusion terms after closure) are included in the model. For the sake of brevity it suffices to say that the model results

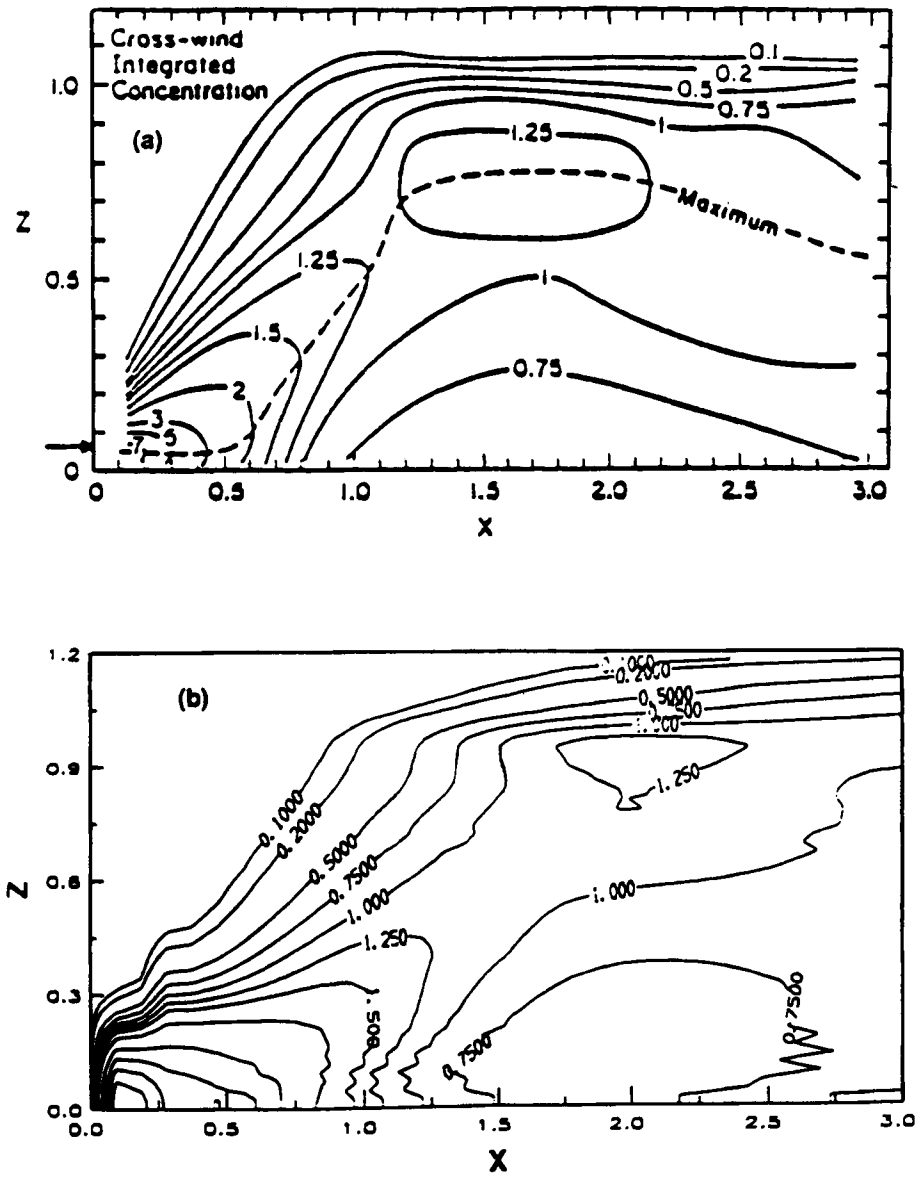

Figure 1. Steady state contours of dimensionless cross-wind integrated concentration as a function of dimensionless downwind distance and dimensionless vertical height from (a) Willis and Deardorff's experiments and (b) the second-order closure model. The source is at 75 m

also capture the plume behaviour of elevated sources in convective boundary layers described in Willis and Deardorff.[3,4]

CONCLUSIONS

In this paper we have demonstrated that the second-order closure model can describe the plume behaviour in convective boundary layers. Furthermore, the time-splitting finite element method

can provide reliable results without having to solve an extremely large sparse matrix for each time step.

ACKNOWLEDGEMENTS

This work was partially supported by the Center for Computational Sciences at the University of Kentucky and the U.S. Army Chemical Research and Development Engineering Center. Computations were performed at the University of Kentucky and the Cornell National Supercomputing Facility.

REFERENCES

1. J. W. Deardorff and G. E. Willis, 'A parameterization of diffusion into the mixed layer', *J. Appl. Meteorol.*, **14**, 1451–1458 (1975).
2. G. E. Willis and J. W. Deardorff, 'A laboratory model of diffusion into the convective planetary boundary layer', *Q. J. R. Meteorol. Soc.*, **102**, 427–445 (1976).
3. G. E. Willis and J. W. Deardorff, 'A laboratory study of dispersion from an elevated source within a modeled convective planetary boundary layer', *Atmos. Environ.*, **12**, 1305–1311 (1978).
4. G. E. Willis and J. W. Deardorff, 'A laboratory study of dispersion from a source in the middle of the convective mixed layer', *Atmos. Environ.*, **15**, 109–117 (1981).
5. M. Poreh and J. E. Cermak, 'Diffusion in an atmospheric layer with an elevated inversion', in R. H. Kohl (ed.), *Proc. 1985 Scientific Conf. on Obscuration and Aerosol Research*, U.S. Army Chemical Research and Development Engineering Center, Aberdeen Proving Ground, MD, 1986, pp. 113–115.
6. W. R. Moninger, W. L. Eberhard, G. A. Briggs, R. A. Kropfli and J. C. Kaimal, 'Simultaneous radar and lidar observations of plumes from continuous point sources', *Preprints 21st Radar Meteorology Conf.*, American Meteorological Society, Boston, MA, 1983, pp. 246–250.
7. R. G. Lamb, 'Diffusion in the convective boundary layer', in F. T. M. Nieuwstadt and H. Van Dop (eds), *Atmospheric Turbulence and Air Pollution Modeling*, Reidel, Boston, MA, 1982, pp. 159–230.
8. J. C. R. Hunt, J. C. Kaimal and J. E. Gaynor, 'Eddy structure in the convective boundary layer—new measurements and new concepts', *Q. J. R. Meteorol. Soc.*, **114**, 827–858 (1988).
9. L. Enger, 'A. higher order closure model applied to dispersion in a convective PBL', *Atmos. Environ.*, **20**, 879–894 (1986).
10. W. Y. Sun, 'Air pollution in a convective boundary layer', *Atmos. Environ.*, **20**, 1877–1886 (1986).
11. W. Y. Sun, 'Numerical study of dispersion in the convective boundary layer', *Atmos. Environ.*, **23**, 1205–1217 (1989).
12. P. Pai and T. H. Tsang, 'A finite element solution to turbulent diffusion in a convective boundary layer', *Int. j. numer. methods fluids*, **12**, 179–195 (1991).
13. W. S. Lewellen and M. E. Teske, 'Second-order closure modeling of diffusion in the atmospheric boundary layer', *Boundary Layer Meteorol.*, **10**, 69–90 (1976).
14. L. Enger, 'Simulation of dispersion in moderately complex terrain—Part B. The higher order closure dispersion model', *Atmos. Environ. A*, **24**, 2447–2455 (1990).
15. J. L. Lumley, 'Computational modeling of turbulent flows', *Adv. Appl. Mech.*, **18**, 123–176 (1979).
16. C. duP. Donaldson, 'Construction of a dynamic model of production of atmospheric turbulence and the dispersal of atmospheric pollutants', in P. A. Haugen (ed.), *Workshop of Micrometeorology*, American Meteorological Society, Boston, MA, 1973, pp. 313–392.
17. W. S. Lewellen and M. Teske, 'Prediction of the Monin–Obukhov similarity functions from an invariant model of turbulence', *J. Atmos. Sci.*, **30**, 1340–1345 (1973).
18. P. E. Long and D. W. Pepper, 'An examination of simple numerical schemes for calculating scalar advection', *J. Appl. Meteorol.*, **20**, 146–156 (1981).
19. G. R. Carmichael, L. K. Peters and T. Kitada, 'A second generation model for regional-scale transport/chemistry/deposition', *Atmos. Environ.*, **20**, 173–188 (1986).
20. D. P. Chock, 'A comparison of numerical methods for solving advection equations—III', *Atmos. Environ. A*, **25**, 853–871 (1991).
21. J. Bartinicki, 'A simple filtering procedure for removing negative values from numerical solutions of the advection equation', *Environ. Softw.* **4**, 187–201 (1989).
22. J. C. Wyngaard and O. R. Cote, 'The evolution of a convective planetary boundary layer—a higher-order-closure model study', *Boundary Layer Meteorol.*, **7**, 289–308 (1974).
23. G. E. Willis and J. W. Deardorff, 'On the use of Taylor's translation hypothesis for diffusion in the mixed layer', *Q. J. R. Meteorol. Soc.*, **102**, 817–822 (1976).